Chapter 1
The Polyol Process

Fernand Fiévet and Roberta Brayner

Abstract Among the chemical, physical, or electrochemical processes generally used in particles production, the polyol-mediated synthesis of inorganic nanoparticles appears as an easy to carry out and versatile route. In this chapter, properties of polyols (α-diols and etherglycols) are first recalled in order to explain the versatility of this process. Guidelines which allow controlling the nucleation and growth steps in such media are then given in order to obtain particles with well-defined characteristics namely, a uniform shape, a mean size in the micron, submicron or nanometer range with a narrow size distribution, and a low degree of agglomeration. Examples of size tuning of ferromagnetic metals (Fe, Co, Ni, and their alloys) and noble metals are given as well as examples of shape control leading to 1D nanostructures with a particulate emphasis on the growth mechanism of silver nanorods or nanowires. Examples of polyol-mediated synthesis of oxide (spinel ferrites, Cu_2O, ZnO) nanoparticles through hydrolysis reaction are also given. Throughout this chapter it is pointed out how the polyol process allows tuning the size and shape-dependent magnetic properties of ferromagnetic metal or spinel ferrite particles which may be used as advanced functional materials in various fields: high permeability composite materials, high density recording media, high temperature permanent magnets, and in biomedical applications such as magnetic resonance imaging, cancer treatment by hyperthermia, or targeted drug delivery

F. Fiévet (✉) · R. Brayner
Laboratoire ITODYS, University of Paris Diderot,
Sorbonne Paris Cité, UMR 7086, 75205 Paris, France
e-mail: fievet@univ-paris-diderot.fr

R. Brayner et al. (eds.), *Nanomaterials: A Danger or a Promise?*,
DOI: 10.1007/978-1-4471-4213-3_1,

1.1 Introduction

Over the recent years, metal, oxide, or semi-conducting nanoparticles have attracted considerable interest because of the size and shape dependence of their electronic, optical, magnetic, or catalytic properties and their potential use as tiny building blocks to make nanocomposite or bulk nanostructured materials. The fine-tuning of such properties for application in various fields such as electronics, photonics, information storage, and biomedicine, often requires the synthesis of non-agglomerated particles with a definite and uniform shape, a given mean size, and a narrow size distribution. Among the chemical, physical, or electrochemical processes generally used in particles production, the chemical ones, in particular those from solution, appear suitable for affording such fine particles with tailored morphological characteristics, if the precipitation, namely nucleation and growth steps, are conducted under kinetically controlled conditions. The polyol-mediated synthesis of inorganic nanoparticles, which was first studied by our group 20 years ago [1–3] and then extensively developed by many other groups as by ours, is able to fulfill these requirements in many cases as exemplified in this chapter for metals and oxides.

1.2 Description of the Polyol Process

1.2.1 Historical Review

The polyol process was described at first as a novel route for preparing finely divided metal powders of easily reducible metals such as copper [4], noble metals namely Au [5], Pd [6], Ag [7, 8], and their alloys [9, 10], or less reducible metals such as cobalt, nickel, iron, and their alloys [2, 3, 11–13] by reduction of inorganic precursors in liquid polyols. Polyols were either polyhydric alcohols namely α-diols such as 1,2-ethanediol (ethylene glycol), 1,2-propanediol (propylene glycol), or etherglycols namely di(ethylene) or tri(ethylene glycol). The solid precursor is suspended in the liquid polyol, which may be quite soluble (nitrate, chloride, acetate) or only slightly soluble (oxide, hydroxide). The solution or the suspension is stirred and heated to a given temperature which can reach the boiling point of the polyol for less reducible metals; conversely, for easily reducible metals (e.g. Pd) the reaction can be carried out at temperature as low as 0 °C. Polyols are interesting among non-aqueous solvents because like water and monoalcohols, they are hydrogen-bonded liquids with a high value of relative permittivity (Table 1.1); therefore they are able to dissolve, to some extent, ionic inorganic compounds. Moreover, polyols, as well as monoalcohols, are mild reducing agents but this reduction can be carried out in such solvents under atmospheric pressure up to 250 °C if necessary. Polyols, such as α-diols, owing to their chelating properties, are also coordinating solvents which can form

Table 1.1 Relative permittivity and boiling point under atmospheric pressure of some polyols comparison with water and monoalcohols

	Water	1,2-ethanediol	1,2-propanediol	Di(ethylene glycol)	Methanol	Ethanol	1-octanol
ε_r	78.5	38	32	32	33	24	10
T_b (°C)	100	198	189	245	65	78.5	194

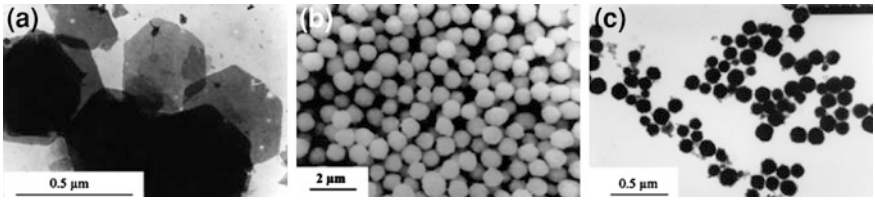

Fig. 1.1 TEM images of different inorganic compounds obtained from $Co(CH_3CO_2)_2{\cdot}4H_2O$: **a** cobalt hydroxyacetate (DEG, $h = 26$, T = 60 °C), **b** cobalt metal (EG/DEG, $h = 0$, T = 200 °C), **c** cobalt(II) oxide (DEG, $h = 4$, T = 185 °C) (*EG* ethylene glycol, *DEG* di(ethylene) glycol, *h* hydrolysis ratio) [19]

complexes with many metal cations. Therefore, they can form reactive intermediate species on one hand, and on the other adsorb onto the surface of the growing particles preventing aggregation.

Later, polyols have also been used to elaborate a large variety of oxides [14–19] and layered hydroxyl salts [20] through forced hydrolysis and inorganic polymerization. The final compound of these reactions depends mainly upon the hydrolysis ratio *h* defined as the ratio between the amount of water added in the polyol and the amount of metal involved as exemplified for cobalt (Fig. 1.1).

More recently, the polyol process has also been used with thiourea or sodium sulfide to prepare sulfide nanoparticles [21–23] or with sodium hydrogen phosphate to obtain phosphates [24, 25]. Finally, the polyol-mediated synthesis appears as a rather simple and convenient route to prepare various nanoscale functional materials [26] through different reactions.

1.2.2 A Versatile Process

Whatever the synthesis carried out in polyols, the reaction occurs via a progressive or total dissolution of the solid precursor rather than solid phase transformation. It is well known that the precipitation of a solid from a solution proceeds in two steps: nucleation and particle growth. During the nucleation step, nuclei are formed by a stepwise bimolecular addition of monomeric entities of the solute. In order to initiate the spontaneous growth of stable particles (growth step) the small aggregates which form the nuclei have to reach a critical size (nucleation step). Therefore, the

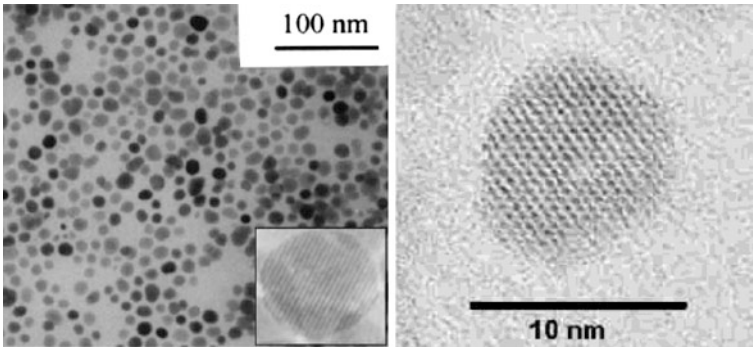

Fig. 1.2 TEM images of ferrite nanoparticles obtained in polyols showing their high crystallinity **a** Zn Fe_2O_4 [35], **b** Mn Fe_2O_4 [36]

morphological characteristics of the final particles, i.e., their size, shape, and degree of aggregation depend upon the relative rates of these two steps. In such a precipitation it is possible to tune these morphological characteristics by acting above numerous experimental parameters. To achieve this goal for a given system, one can act at first upon the reactants (nature and concentration of the solid precursor, nature of the polyol, pH of the solution) and the way they are brought together (progressive injection by a syringe pump to achieve a better control upon nucleation and growth for instance [27]). One can also act upon the heating conditions (temperature ramping rate and final temperature for usual heating, microwave heating) and the duration of reaction. If polyols are able to control the growth of the particles to some extent and to prevent their agglomeration by coordinating onto their surfaces, it may be useful in some cases, namely for the synthesis of noble metals, to add polymeric protective agents such as poly (vinylpyrrolidone) (PVP) for instance [7, 8, 27] or surfactants such as oleic or lauric acid [28]. For the preparation of metal nanoparticles the seeding of the reaction medium by foreign nuclei (heterogeneous nucleation) provides an efficient tool to steer the average size of spherical particles in a large size range [29]; it also allows in some particular cases to obtain nanoparticles of various shapes, [30] namely nanorods [31] or nanowires [32, 33].

For the polyol-mediated synthesis of oxides a defined amount of water has to be added into the polyol and the relative concentration of water versus the metal concentration, i.e., the hydrolysis ratio, is a critical parameter [16, 21] to tune the size of the nanoparticles obtained through spontaneous nucleation (homogeneous nucleation). One of the interesting characteristics of the so-obtained oxide nanoparticles is their surprisingly good crystallinity. For instance, of the various methods of fabricating ferrite nanoparticles, the forced hydrolysis of metal salts in polyol appears as an attractive soft chemistry route carried out under temperature close to hydrothermal conditions which then provides very well-crystallized nanoparticles showing enhanced magnetic characteristics (Fig. 1.2) [17, 34–36]. But, like other soft chemistry routes, it sometimes allows obtaining metastable phases such as for instance CoO or solid solutions ZnO–CoO with a high Co content [18].

Moreover, whatever the targeted nanoparticles, metals, oxides, or chalcogenides the polyol-mediated synthesis is rather easy to perform at laboratory scale. The reaction rate can be drastically increased under microwave heating as evidenced in the previous years [37]. It has also been shown that it is possible to scale up the production of the nanoparticles by replacing the conventional batch production by a continuous process, where the solvent and precursors are fed continuously [38, 39]. Altogether, the polyol process appears to be a versatile route suitable for the preparation of particles of a number of particulate inorganic compounds (elemental metals, oxides, chalcogenides) in a large size range and namely at the nanometer scale.

1.3 Control of the Size and Shape of the Particles in Polyols

1.3.1 Guidelines

Generally, metal, oxide, or chalcogenide particles obtained through precipitation in polyols show well-defined characteristics: a uniform shape often almost spherical, a rather narrow size distribution with a mean diameter either in the micron, submicron, or nanometer size range, and small degree of aggregation. The formation of bulk solids is always thermodynamically favored over the formation of small particles with a large surface area and many incompletely coordinated surface sites. Agglomeration of the particles is also thermodynamically favored for the same reason. Therefore, to obtain such well-defined characteristics two general conditions must be fulfilled: nucleation and growth must be two completely separated steps according to the model of LaMer and Dinegar [40] and coalescence of the particles must be prevented.

1.3.1.1 Control of the Nucleation Step

Metals, oxides, or chalcogenides are only sparingly soluble in polyols. The saturation level is low and spontaneous nucleation occurs when the concentration of the species generated by the reduction or hydrolysis reactions reaches a critical supersaturation level. If the final compound is generated slowly and the nucleation rate is high enough, then the sudden nucleation lowers almost immediately the concentration below this critical nucleation level. Under these conditions the nucleation step is very brief and is followed by the growth of particles from the original nuclei as long as the final compound is slowly generated as the concentration remains higher than the saturation one (Fig. 1.3a). Nucleation rate increases sharply versus concentration above the critical nucleation threshold, whereas growth rate increases slowly above the saturation concentration (Fig. 1.3b). To prevent further nucleation during the growth step supersaturation

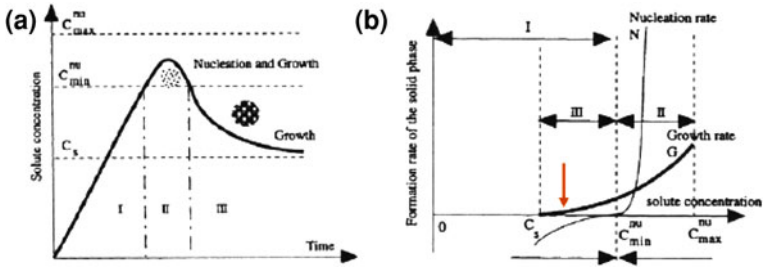

Fig. 1.3 **a** Nucleation and growth according to LaMer's model [40], **b** comparison of nucleation and growth rates versus concentration of the final compound in solution

must remain at a low level. This can be achieved by different methods. Starting from a very soluble precursor the reaction of formation of the final solid compound from the solution has to be carried out at a sufficiently low temperature. When various soluble precursors may be used one can select the most suitable one. In other cases it is possible to control the concentration of the precursor species in solution, these species being provided by the progressive dissolution of a sparingly solid phase (starting compound or intermediate solid phase) acting as a kind of reservoir. The dissolution equilibrium regulates the release of these species, controls the supersaturation ratio, and then allows having a very brief nucleation step. Nevertheless, it is possible to have an important yield at the end of the growth despite the low supersaturation ratio. In some cases, to achieve more easily the separation between the nucleation and growth steps and a better control of the average size of the final particles, homogeneous (spontaneous) nucleation can be replaced by heterogeneous nucleation by seeding the reactive medium with foreign nuclei obtained by adding a suitable nucleating agent.

1.3.1.2 Growth and Stabilization of Particles

Particles growth may proceed either by diffusion of the solute species toward the surface of the particles and stepwise addition of atoms or ions (Fig. 1.4a), or by coalescence of primary particles which form secondary larger particles (Fig. 1.4b).

Coalescence of primary particles usually results in uncontrolled growth leading to polydisperse secondary particles of various shapes. Thus, to obtain particles with well-defined morphological characteristics it is generally necessary to prevent the coalescence of the particles during their growth stage. This can be achieved by either steric or electrostatic stabilization. Steric stabilization can be provided by the polyol itself or by adding long-chain molecules. The adsorption of such protective agents can also be used to limit the growth if necessary in order to obtain nanoparticles. Electrostatic stabilization can be provided by carboxylate anions, namely acetate ions, when such metallic salts are used as starting compounds. Nevertheless, it must be pointed out that in some particular cases the formation of

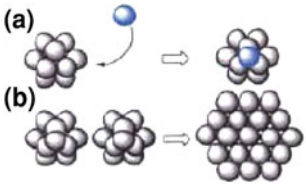

Fig. 1.4 **a** Growth by stepwise addition of atoms or ions; **b** growth by coalescence of primary particles

quasi-spherical secondary metal particles with a rather narrow size distribution through a coalescence mechanism has been evidenced [41]. It is also noteworthy that even when polydisperse nanoparticles are obtained in the early stages of the precipitation due to uncontrolled growth, it has been shown in some cases that final particles with a narrow size distribution can be obtained by a further growth of particles having larger sizes at the expense of smaller ones through Ostwald ripening [42].

A kinetic control of the nucleation and growth steps allows in certain systems to control the shape of the particles and to induce an anisotropic growth which generates 1D nanostructures such as nanorods or nanowires. Such syntheses have been carried out in polyols for metals which crystallize with a highly anisotropic crystal lattice such as *hcp* Co or Co–Ni alloys and also for metals which crystallize in the highly symmetric cubic lattice such as Ag (cf. Sects. 3.2.2 and 3.3.2).

1.3.2 Synthesis of Ferromagnetic Metal Nanoparticles

The magnetic properties of particulate ferro or ferrimagnetic materials are strongly dependent on elemental composition, particle shape and size, and species adsorbed onto the surface. This is especially true for micro and nanosized samples comparable to the domain length scale. The first attempts to achieve a polyol-mediated synthesis of metal particles with well-defined morphological characteristics were carried out with ferromagnetic metals Fe, Co, Ni, and their alloys [2, 3, 11–13]. As long as the nucleation is spontaneous, particles with a uniform quasi-spherical shape and a narrow size distribution were obtained in the micron and submicron range whatever their composition (Fig. 1.5).

Starting from cobalt or nickel acetates dissolved in polyols, the key for the formation of uniform particles was believed to be the formation upon heating of solid intermediate phases such as metallic hydroxyacetates or alkoxides (Fig. 1.6). Sodium hydroxide was added in the polyol in order to favor the formation of these phases which act as a reservoir for the metal solvated cations prior to their reduction into metal. Such a control of the metallic species concentrations allows making monodisperse metal particles through a control of the growth step of these particles which favors its separation from the nucleation one.

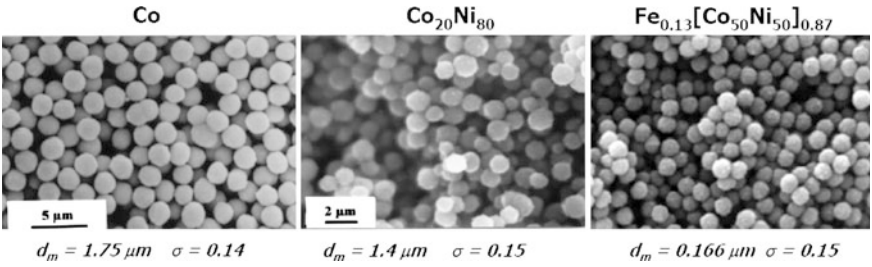

Fig. 1.5 SEM images of ferromagnetic metal particles obtained in polyols through spontaneous nucleation (d_m: mean diameter; σ: relative standard deviation)

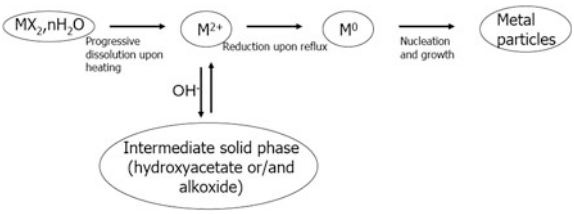

Fig. 1.6 Control of the growth of Co, Ni, and CoNi particles in polyols through the kinetics of dissolution of intermediate solid phases which act as a cation reservoir

1.3.2.1 Size Tuning

An accurate and reproducible control of the mean diameter of the particles can be achieved in the submicrometer and nanometer size ranges as well, by heterogeneous nucleation. As cations of noble metals such as Ag, Pt, or Ru are easily reduced by polyols, the seeding of the reaction medium was achieved using a soluble precursor such as $AgNO_3$, K_2PtCl_4, or $RuCl_3$ in order to generate in situ at low temperature numerous metal nuclei which then acted as suitable sites for the further growth of the ferromagnetic metal particles under reflux. Thus, the separation of nucleation and growth steps is easily achieved favoring the formation of monodisperse particles. An accurate and reliable control of their mean diameter is obtained by varying the ratio of the noble metal concentration to that of ferromagnetic metals in the range 10^{-2}–10^{-5} (Fig. 1.7).

Such samples have been used as model materials to study the evolution of the dynamic properties of fine particles with their size [13] and as components to make high permeability composite materials [11].

A few years ago, Jeyadevan's group succeeded in synthesizing submicron-sized Fe particles in a concentrated NaOH solution in ethylene glycol [43]. Moreover, they obtained recently through heterogeneous nucleation, using H_2PtCl_6 as nucleating agent, size-controlled Fe nanoparticles ranging between 90 and 10 nm with a cubic morphology above 25 nm, the smaller one being spherical and agglomerated (Fig. 1.8). The as-prepared 60 nm-sized particles are protected from oxidation in air by a biocompatible oxide layer. Their biocompatibility and their

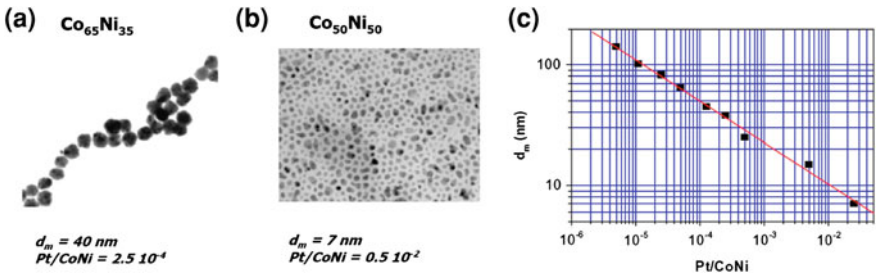

Fig. 1.7 **a**, **b** TEM images of CoNi alloys nanoparticles obtained in polyols through heterogeneous nucleation by generating in situ Pt nuclei, **c** accurate control of the mean size of CoNi particles by varying Pt concentration

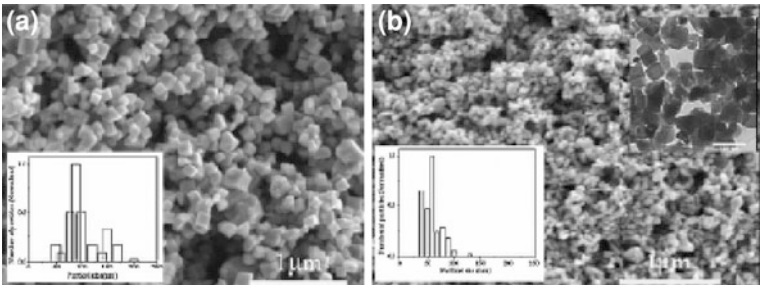

Fig. 1.8 SEM images of Fe nanocubes obtained in NaOH ethylene glycol solution from $FeCl_2.4H_2O$ through heterogeneous nucleation using H_2PtCl_6 as nucleating gent at different concentrations **a** 5×10^{-9} M, **b** 1×10^{-8} M. Particle size distribution in bottom insets, TEM image in top inset [44]

high saturation magnetization offer a potential advantage for biomedical applications such as targeted drug delivery [44]. Nanoparticles of Fe-based alloys such as FeCo [45] and Fe Pt [46] were synthesized by Jeyadevan's group as well. It must be pointed out that it is possible to synthesize by a modified polyol method equiatomic FePt nanoparticles with the $L1_0$ ordered structure without any subsequent annealing. Such nanoparticles whose diameters are 5–10 nm appear as promising candidates for ultra high density magnetic recording media due to their very large magnetocrystalline anisotropy.

1.3.2.2 Shape Control Toward 1D Nanostructure

Magnetic nanorods or nanowires have a high shape anisotropy which provides high coercivity. Despite a diameter in the nanometer range, ferromagnetic properties are observed at room temperature since the blocking temperature increases

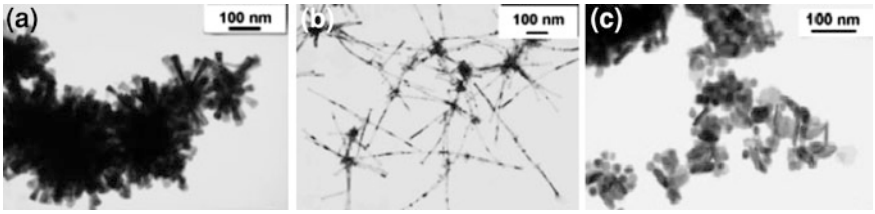

Fig. 1.9 TEM images of $Co_{80}Ni_{20}$ particles prepared by reduction of cobalt and nickel acetates in NaOH solution in 1,2-propanediol upon seeding with Ru with various hydroxide concentrations **a** 0.05 mol L^{-1}; **b** 0.15 mol L^{-1}; **c** 0.2 mol L^{-1} [32]

with the aspect ratio. Self-organized nanowires may find applications in high density magnetic recording [47]. Moreover, aligned nanowires or nanorods of hard magnetic materials were expected to provide an original "bottom up" fabrication method for macroscopic permanent magnets [31]. In this context several methods have been used for anisotropic growth of metal nanoparticles such as use of solid host templates [48] and templating effect of surfactant molecules through a self-organization process during the hydrogenation of organometallic compounds [47]. In the polyol-mediated synthesis of metals the first example of anisotropic growth was observed in the presence of poly(vinyl pyrrolidone) with silver particles obtained by heterogeneous nucleation upon seeding with platinum nuclei [7, 33]. Further, it was shown that anisotropic CoNi particles can be prepared by reduction of acetate in 1,2-propanediol with addition of various amounts of sodium hydroxide (Fig. 1.9). The key to obtain nanowires in a narrow hydroxide concentration range was the seeding with ruthenium nuclei with a high nucleating ratio [Ru]/[Co + Ni] = 2.5 mol% [32]. It was also observed that the particles' shape depends strongly upon the Co/Ni composition of the particles, wires being obtained only with cobalt content higher or equal to 50 at-%, whereas for nickel only platelets being obtained (Fig. 1.10) [49]. Increasing the sodium hydroxide concentration lowers the Co^{2+} and Ni^{2+} concentrations through the precipitation of intermediate solid phases which are alkoxide and hydroxy-acetate for Co and Ni respectively. These different solid phases suggest that the molecular complexes of Co(II) and Ni(II) in solution are distinct. These differences in coordination chemistry can explain the different behaviors of the two metals toward reduction. Different dissolution rates of the two solid phases and different reduction rates in solution for molecular species of a different nature are expected. The various shapes can be explained by nucleation and growth rates controlled both by the cobalt/nickel composition and sodium hydroxide concentration suggesting that the nanowires are obtained with a higher growth rate than the platelets.

In order to get optimized building blocks for the "bottom up" fabrication of macroscopic permanent magnets the synthesis of highly crystalline Co *hcp*-isolated nanorods with a high aspect ratio is required. In such materials the high magnetocrystalline anisotropy due to the highly anisotropic crystal lattice and the shape anisotropy would give high coercivity and remanent magnetization.

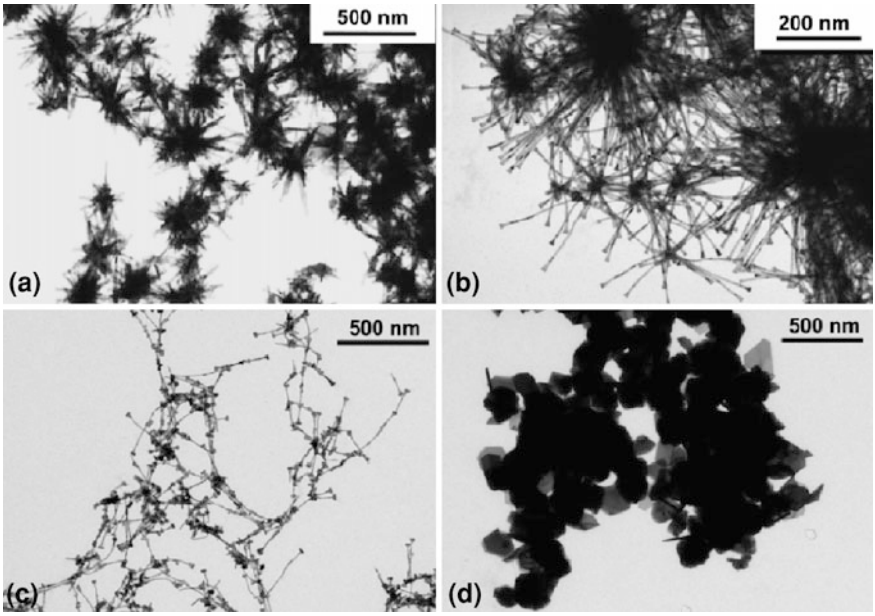

Fig. 1.10 TEM images of CoNi particles prepared by reduction of cobalt and nickel acetates in a 0.1 M NaOH solution in 1,2-propanediol: **a** Co wires; **b** $Co_{80}Ni_{20}$ wires; **c** $Co_{50}Ni_{50}$ wires; **d** Ni platelets [49]

Such a synthesis has been carried out by reduction of carboxylate salts of Co^{II} in 1,2-butanediol (BEG) [31]. By choosing the proper carboxylate counterions and varying the hydroxide concentration it is possible to change the nature of the intermediate solid phase, to adjust the concentration of the reducible Co^{II} species, to control the growth rate of the Co nanoparticles to favor an anisotropic growth, and finally to obtain rods with desired diameter and aspect ratio (Figs. 1.11, 1.12, and 1.13). Pressed powders and magnetically oriented samples made up with such nanorods exhibit a high coercivity and have the suitable properties to realize "high temperature magnets" competitive with AlNiCo or SmCo permanent magnets. They could also be used as recording media for high density magnetic recording [50].

1.3.3 Synthesis of Noble Metal Nanoparticles

Noble metal nanoparticles can be synthesized by many chemical methods using different reducing agents and solvents. Long ago, shape control has received considerable attention for silver and gold nanoparticles which have numerous applications in surface plasmons, surface enhanced Raman spectroscopy (SERS),

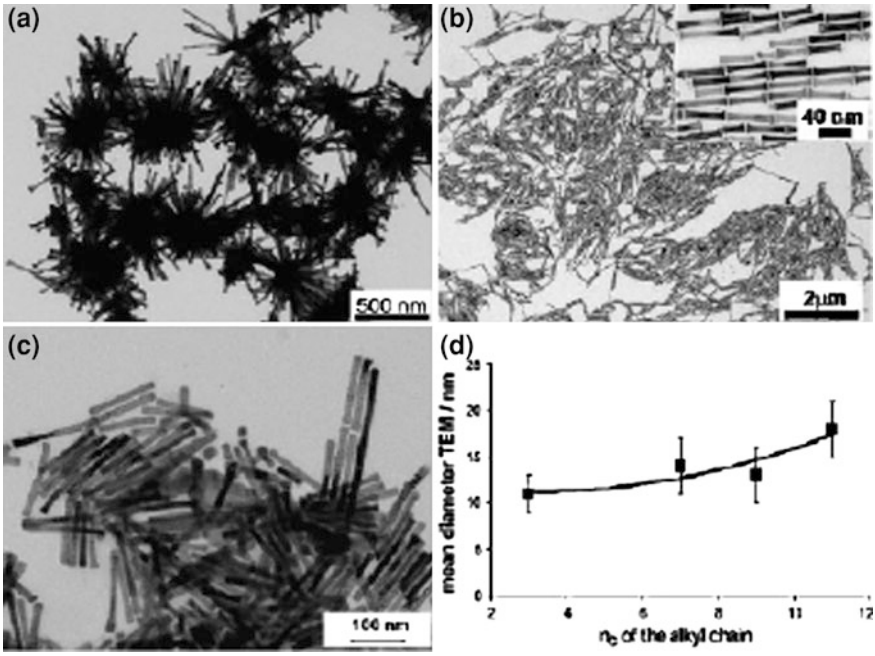

Fig. 1.11 TEM images of Co particles obtained by reduction of different carboxylates in BEG **a** sea-urchin-like particles from Co acetate, **b** nanorods ($L_m = 99$ nm, $\sigma_{Lm}/L_m = 17$ %; $d_m = 15$ nm, $\sigma_{dm}/d_m = 9$ %) from laurate, **c** nanorods from cobalt caproate ($n_c = 5$). **d** Influence of the length of the carboxylate carbon chain on d_m of the nanorods [31]

or as biological sensors. It was shown early that polyols can be used both as mild reducing agents and solvents to obtain particles of noble metals (Au, Pd, Ag) or alloys (AgPd) [5–10]. In contrast to the synthesis of ferromagnetic metal particles, this can be carried out at temperature lower than the boiling point, without formation of solid intermediate phases but with addition of a protective agent such as PVP to prevent the strong tendency of fine metal particles to coalesce. In these first studies it was shown that nanoparticles with a uniform spherical shape, a few nanometers in size, and a narrow size distribution can be obtained with Ag [8] and Pt-group metals as well [51]. It was possible to gain a first insight into the reaction mechanism for the synthesis of silver nanoparticles, the size homogenization of the particles resulting from Ostwald ripening [52]. Moreover, it was evidenced that silver rods particles can be obtained through heterogeneous nucleation with platinum nuclei formed in situ [7]. During the last decade good progress has been made in the control of size, shape, and surface capping in the synthesis of noble metal nanoparticles and in the understanding of the growth mechanism as exemplified in the following two sections.

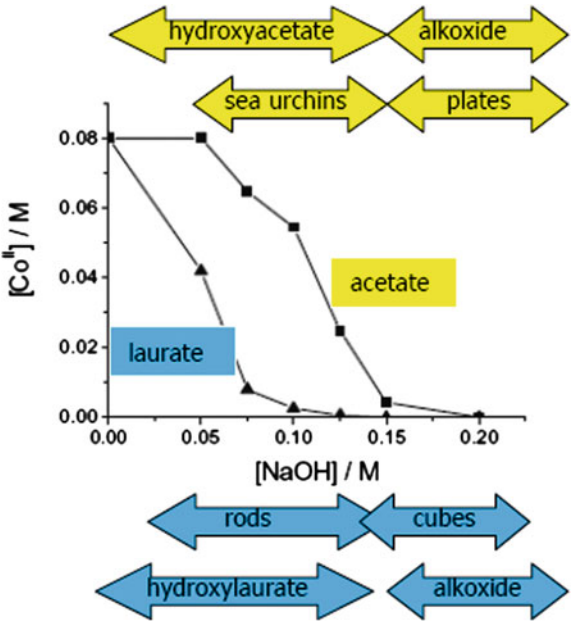

Fig. 1.12 [Co^{II}] in basic solution of BEG immediately before reduction, nature of the intermediate solid phase, and shape of the final particles versus [NaOH] using the acetate and laurate precursors

1.3.3.1 Ruthenium Nanoparticles: Size, Shape, and Self-assemblies

Monodisperse ruthenium nanoparticles were obtained from $RuCl_3$ from acetate solution in polyols [53]. Due to their strong affinity for such particles acetate ions added in sufficient amount are found to be the best way to prevent agglomeration through electrostatic stabilization. The mean diameter of the particles is tuned reproducibly in the 1.5–6 nm range by varying the synthesis temperature and the acetate concentration, a very narrow size distribution being observed in the whole sample without any further size selection processes (Fig. 1.14a, b and Table 1.2). The higher the temperature the higher the nucleation rate, and for a given concentration of metal, the lower the mean particle size. Nucleation and growth rates depend upon [AcO-]/[Ru] ratio because acetate ions can act as ligands for both the metal particles and the Ru(III) and Ru(II) species in solution. Among a majority of nearly isotropic particles, a significant number of platelets with an aspect ratio as low as ¼ is observed.

For samples with the lowest size standard deviation self-organization of particles coated with dodecane thiol can be observed on the carbon membrane of the TEM grid. Depending upon thiol concentration columnar units made of edgewise stacked platelets or hexagonal arrays of isotropic particles juxtaposed with a mean interparticle distance of 2 nm are evidenced (Fig. 1.14c–d). Close-packed or non compact stacking of two hexagonal layers are observed depending on the evaporation rate of the solvent.

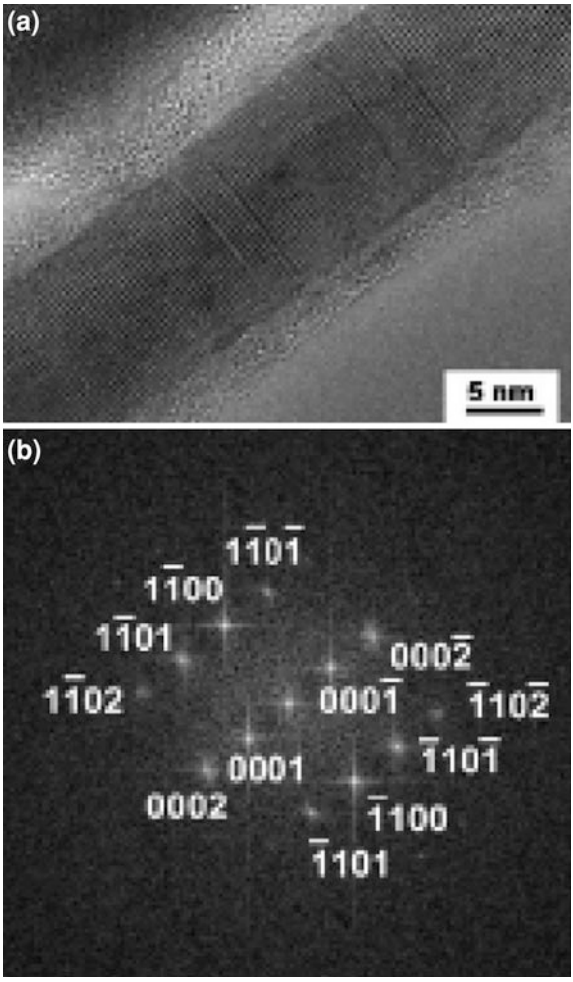

Fig. 1.13 **a** HRTEM image of a single *hcp* cobalt rod with the *c* axis parallel to the rod axis, **b** the corresponding numerical diffraction pattern. [31]

1.3.3.2 Growth Mechanism and Shape Control of Silver Nanoparticles

During the last decade Xia's group made several modifications to the early protocol used in the polyol-mediated synthesis of silver particles in order to achieve a better control over the nucleation and growth steps [27]. This allows for the reproducible preparation of nanoparticles of different well-defined and controllable shapes such as nanocubes, nanowires, or nanospheres by simply varying the concentration of the starting compound ($AgNO_3$) and the relative amount of PVP used as capping agent.

A growth mechanism which accounts for these different morphologies has been proposed. Formation of metal clusters and seeds of different crystallinities have been evidenced [54, 55]: (i) single crystal (SC) cuboctahedra with {111} and

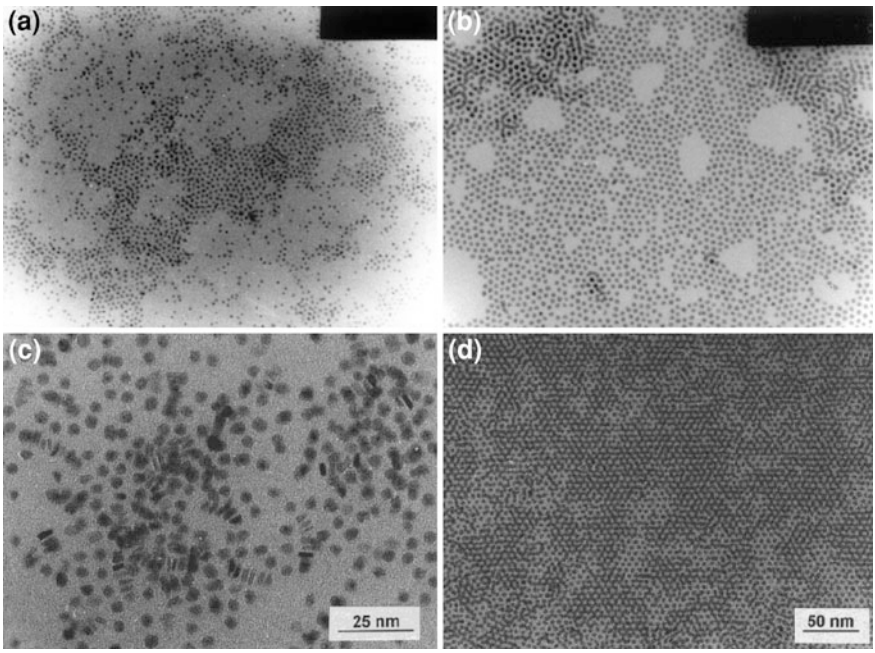

Fig. 1.14 TEM images of ruthenium nanoparticles prepared in sodium acetate solution in 1,2-propanediol **a** $d_m = 2{,}5$ nm $\sigma/d_m = 0.11$, **b** $d_m = 3.95$ nm $\sigma/d_m = 0.066$, **c** lines of a few 4-nm sized platelets particles, **d** mono and bi layer showing compact stacking [53]

Table 1.2 Dependence of the mean diameter and size distribution of Ru nanoparticles obtained in 1,2-propanediol on temperature and acetate concentration [53]

Reaction time (min)	T (°C)	Acetate (mol L^{-1})	d_m (nm)	σ (nm)	σ/d_m
10	165	$1.1\ 10^{-2}$	1.6	0.24	0.15
10	165	$2.2\ 10^{-2}$	1.4	0.18	0.13
10	165	$4.4\ 10^{-2}$	1.8	0.18	0.10
10	150	$1.0\ 10^{-2}$	3.95	0.26	0.066
10	150	$2.0\ 10^{-2}$	1.7	0.21	0.12
10	150	$4.0\ 10^{-2}$	2.0	0.25	0.125
10	150	$8.8\ 10^{-2}$	2.5	0.28	0.11
30	140	$1.0\ 10^{-2}$	6		
30	140	$2.0\ 10^{-2}$	2.2		

{100} facets, (ii) multiply-twinned particles (MTP) often in the decahedral shape with {111} facets only, (iii) quasi-spherical multiply-twinned particles. The control of the shape of the final particles is tentatively explained as follows. MTP decahedra seeds are the most thermodynamically stable ones since they are bond only by {111} facets which have the lowest energy. Nevertheless, if nucleation and growth are fast enough the available time for twin defects to form is short and the

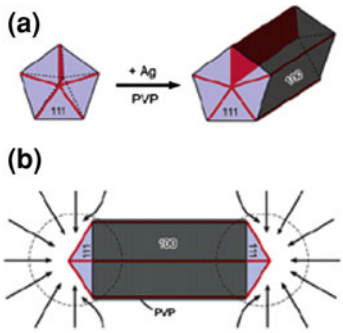

Fig. 1.15 Growth mechanism of pentagonal silver nanowires: **a** growth of a nanorod from an MTP decahedral seed with limited access of silver atoms to {100} facets due to selective adsorption of PVP, **b** diffusion of silver atoms the two ends of a nanorod [54]

formation of SC cuboctahedra seeds is kinetically favored. By varying the [PVP]/[$AgNO_3$] ratio the thickness of the PVP layer and the location of the polymer chains could be modified due to a preferential adsorption onto the {100} facets. Thus, the growth rates of the different facets can be tuned and nanoparticles with distinct shapes can be obtained. Nanocubes are the result of a kinetically controlled growth from SC cuboctahedra; pentagonal nanowires the result of a twin-induced anisotropic growth from MTP decahedra (Fig. 1.15), and nanospheres the result of an isotropic growth of MTP seeds coated with a thick PVP layer on each facet. This mechanism is consistent with many experimental features evidenced by Xia's group, namely the influence upon morphology of trace amounts of inorganic species such as chloride ion and oxygen which promote the formation of single crystal truncated cubes and tetrahedron [55] or CuCl or $CuCl_2$ which favor the rapid synthesis of nanowires [56]. Moreover, according to the same guidelines shape control of nanoparticles has been achieved with platinum and palladium as well [57, 58].

1.3.4 Synthesis of Oxide Nanoparticles

The first report on the elaboration of oxide particles in polyol deals with the synthesis of zinc oxide from acetate dihydrate in di(ethylene glycol) [14, 59]. Single nanocrystals or monodisperse submicrometer polycrystalline particles formed by aggregation of small crystallites were obtained depending upon the precursor concentration. A plausible mechanism was proposed where acetate ions play two main roles. They deprotonate partially the polyol leading to alkoxy groups and they act as a complexing agent toward the cation with formation of an alkoxyacetate complex, such an alkoxyacetate complex being indeed isolated and characterized [60]. Then the forced hydrolysis occurs upon reflux with the progressive development of ZnO nuclei and crystal growth via olation and oxolation reactions. Such a mechanism is similar to that occurring in the well-known sol–gel process [61], where the alkoxyacetate is formed by addition of acetic acid to an

alcohol solution containing the alkoxide instead to be formed in situ in the described polyol-mediated synthesis.

Since this pioneer work Feldmann's group have extended the polyol route to the synthesis of various oxides to obtain nanoscale functional materials such as luminescent materials (phosphor host lattices: e.g. Y_2O_3), color pigments ($CoAl_2O_4$, Cr_2O_3, $ZnCo_2O_4$, $Ti_{0.85}Ni_{0.05}Nb_{0.10}O_2$), transparent conductive oxide ($ZnO:In^{3+}$), and catalytically active oxides (CeO_2, Mn_3O_4, V_2O_5) [26]. Stable colloidal suspensions of almost non-agglomerated nanoscale particles 30–200 nm in size were obtained from a suitable metal precursor (acetate, alcoholate, halogenide) in di(ethylene glycol). The solid content can be up to 20 %.

Simultaneously, during the past decade Ammar's group used the polyol process to synthesize nanoparticles of spinel-like oxides such as Fe_3O_4, γFe_2O_3, and ferrites MFe_2O_4 (M = Co, Ni, Zn, Mn) in order to tune and optimize their magnetic properties for different applications such as high density magnetic recording [17, 62, 63], high frequency applications [34, 35, 64], biomedical ones (targeted drug delivery, magnetic resonance imaging [65], and cancer treatment by magnetic hyperthermia [66, 67]. Nanoparticles of a few nanometers' size are currently obtained; they have a good crystallinity and a high saturation magnetization with a distribution of the cations on the two sites of the spinel structure which may differ from that of corresponding bulk materials and varies with the particle size [68]. Not very long ago intensive research has focused on the polyol-mediated synthesis of cuprous oxide with the aim to control particles size and shape in order to optimize the electrochemical performance of this material as a lithium-ion battery anode [69–72]. Whatever the nanoparticulate oxide synthesized, the polyol acts as a solvent, a complexing and capping agent which limits particle growth and prevents agglomeration almost always without addition of other additives. Furthermore, the used polyols are weak stabilizers which can be removed easily through surface chemistry exchange induced by specific functional groups. In particular cases the polyol acts also as a reducing agent, for instance when Fe_3O_4 and Cu_2O particles are obtained from Fe(III) and Cu(II) precursors respectively.

Conversely to metal nanoparticles synthesis, oxide nanoparticles are always obtained through spontaneous nucleation without seeding with foreign nuclei. Many experimental factors can modify the size, shape, or crystallinity of the particles. A tuned precursor has to be selected but for a given precursor the characteristics of the particles may depend upon the nature of the polyol as exemplified in Fig. 1.16. The relative amount of water added defined by the hydrolysis ratio can affect the nature of the final compound (Sect. 2.1) but for a given oxide it can affect the particle size as well by acting upon the reflux temperature (Fig. 1.17). An increase in the temperature leads to larger particles but at a defined temperature the particle diameter can be steered by adjusting the duration of the reaction. In particular cases, varying the basicity of the polyol solution by adding sodium hydroxide or sodium acetate can lead to particles of different shapes [73]. The potentiality of the polyol process to synthesize monodisperse oxide nanoparticles with an accurate and reliable mean size and with controlled shapes will be exemplified by some examples in the following sections.

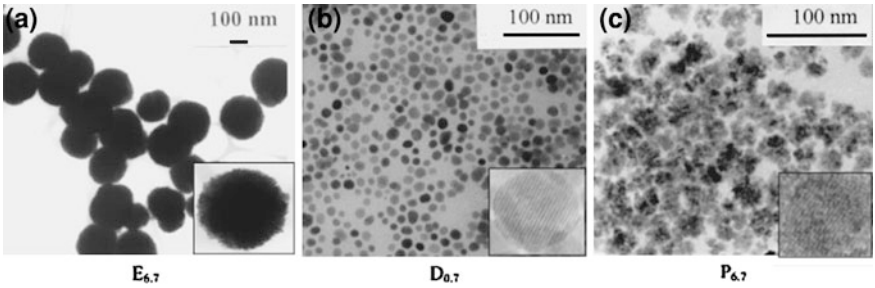

Fig. 1.16 TEM images of $ZnFe_2O_4$ particles obtained from $Zn(CH_3CO_2)_2.2H_2O$ in different polyols under reflux **a** ethylene glycol, $h = 6.7$, **b** di(ethylene glycol), $h = 0.7$, **c** propylene glycol, $h = 6.7$, in inset the HRTEM image of **a** an isolated polycrystalline particle, **b**, **c** a single crystal [35]

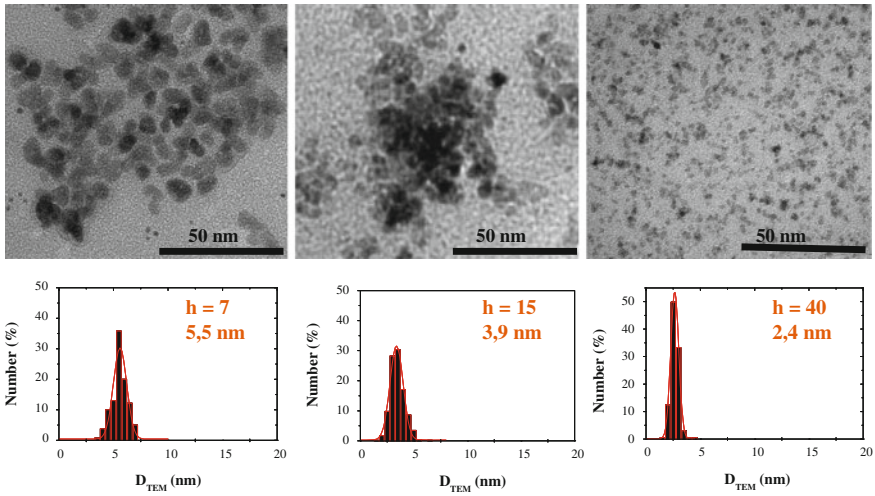

Fig. 1.17 TEM images of $CoFe_2O_4$ samples obtained in DEG under reflux with different amount of water added. The mean diameter decreases when the hydrolysis ratio h increases since the reflux temperature is lowered

1.3.4.1 Size Control of Magnetic Particles for Biological Applications

Colloids of superparmagnetic nanoparticles are promising materials for various biomedical applications, namely magnetic resonance imaging (MRI) and cancer treatment by hyperthermia. Such applications require monodisperse, highly crystalline, chemically stable particles to provide high and reliable magnetization values. Moreover, they must be water soluble and have a low toxicity to ensure good biocompatibility. Currently, superparamagnetic iron oxide nanoparticles (*SPIONs*), Fe_3O_4 (magnetite) and γ-Fe_2O_3 (maghemite) used in biomedicine are obtained by

coprecipitation of iron salts in aqueous solution. Such a method does not ensure a simultaneous control over size and crystallinity and therefore the control of the magnetic properties needs post-size selection process or/and thermal treatment. Alternatively, thermal decomposition of metal organic precursors in high boiling organic solvents with stabilizing ligands leads to highly crystalline, size-controlled monodisperse particles, but requires a post treatment to remove the stabilizing ligands. Recently, *SPIONs* with suitable characteristics have been obtained by the polyol process without the drawbacks of these previous methods. The synthesis of magnetite nanoparticles was carried out by Wan et al. by reacting iron (III) acetylacetonate in tri(ethylene glycol) at elevated temperature without any surfactants [74]. The particles (8 ± 1.1 nm) are superparamagnetic at room temperature. The high reaction temperature favors a high crystallinity and a high magnetization, the particles being stable in aqueous solution or in physiological buffer due to their surface coating by the polyol. Magnetite and maghemite nanoparticles have been obtained by Basti et al. [65] by refluxing Fe(II) acetate solution in di(ethylene glycol) with a hydrolysis ratio equal to 1 and 11 respectively. In order to stabilize the particles in a physiological environment the as-prepared particles were transferred to an aqueous medium through ligand exchange chemistry of the adsorbed polyol species with the dopamine or the catechaldehyde. As expected from the characteristics of these particles (mean size, hydrodynamic radius of coated particles, magnetic characteristics), in vitro resonance imaging essays have shown that they are clearly strong negative contrast agents.

To be used as potential agents for hyperthermia, superparamagnetic nanoparticles must be able to induce selective death of tumoral cells upon heating in the temperature range $42\ °C < T < 47\ °C$. Their efficiency depends strongly upon the average size of the particles and increases sharply when the standard deviation decreases. Therefore, monodisperse particles with a given optimal size and a high magnetization at the body temperature are required. Moreover, a Curie temperature just higher than the therapeutic temperature range would ensure a self-regulated temperature control in an alternating field.

For such an application stoichiometric $Mn_{0,2}Zn_{0,8}Fe_2O_4$ monodisperse nanoparticles were obtained by Ammar's group [67] by forced hydrolysis in di(ethylene glycol) (Fig. 1.18). As Zn-substituted MFe_2O_4 (M : Ni, Co, Fe, Mn) nanoparticles have interesting temperature-sensitive magnetic properties that can be tuned through their chemical composition and cation distribution, a systematic study was then undertaken on $M_{1-x}Zn_xFe_2O_4$ samples varying the cation M, the composition x, and the nature of the polyol with two targeted mean particle sizes (4 and 10 nm) [66]. Table 1.3 exemplifies the potentiality of the polyol process to synthesize monodisperse nanoparticles with a finely tuned size. In some particular cases the polyol process also allows to obtain particles of different shapes as exemplified in the following section.

1.3.4.2 Oxide Particles of Various Shapes

In the past years several groups have focused on the shape control of cuprous oxide polyol-mediated nanoparticles. Park et al. reported on the gram scale synthesis of Cu_2O nanocubes from copper (II)acetylacetonate in 1,5 pentanediol with addition

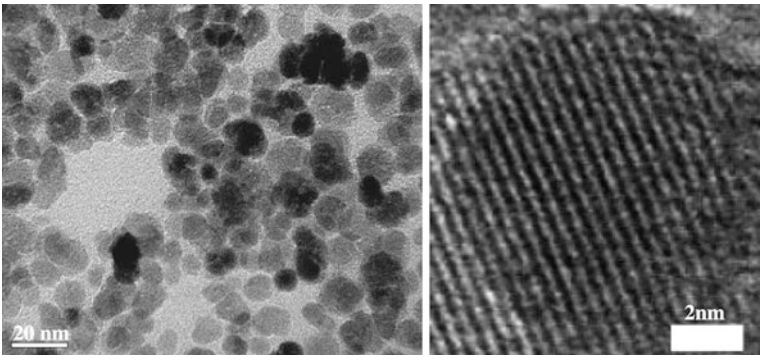

Fig. 1.18 TEM image (*left*) and HRTEM image (*right*) of $Mn_{0,2}Zn_{0,8}Fe_2O_4$ nanoparticles obtained from iron chloride, manganese, and zinc acetates in di(ethylene glycol) under reflux [67]

Table 1.3 Mean particle size and standard deviation inferred from TEM image analysis for various samples prepared in di(ethylene glycol) or tetra(ethylene glycol) with a target size of 4 nm (samples labeled P) or a target size of 10 nm (samples labeled G) [66]

Sample	M	Composition	<D > /nm
PNi1	Ni	$Ni0.1Zn0_{.9}Fe_2O_4$	3.5 ± 0.4
G_{Ni1}			9.5 ± 1.6
P_{Ni2}		$Ni_{0.2}Zn_{0.8}Fe_2O_4$	3.6 ± 0.3
G_{Ni2}			8.3 ± 1.1
P_{Co1}	Co	$Co_{0.1}Zn_{0.9}Fe_2O_4$	4.1 ± 0.5
G_{Co1}			10.9 ± 1.5
P_{Co2}		$Co_{0.2}Zn_{0.8}Fe_2O_4$	4.3 ± 0.5
G_{Co2}			10.3 ± 1.4
P_{Fe1}	Fe	$Fe_{0.1}Zn_{0.9}Fe_2O_4$	4.4 ± 0.5
G_{Fe1}			11.5 ± 1.7
P_{Fe2}		$Fe_{0.2}Zn_{0.8}Fe_2O_4$	4.3 ± 0.5
G_{Fe2}			12.5 ± 1.5
P_{Mn1}	Mn	$Mn_{0.1}Zn_{0.9}Fe_2O_4$	4.1 ± 0.4
G_{Mn1}			10.7 ± 1.1
P_{Mn2}		$Mn_xZn_{1-x}Fe_2O_4$	4.0 ± 0.4
G_{Mn2}		$0.1 < x < 0.2$	11.7 ± 1.8

of PVP [72]. The as-obtained highly monodisperse cubes with an average edge size of 53 ± 3 nm ($\sigma = 6$ %) are single crystals. Their controlled oxidation leads to CuO hollow cubes, hollow spheres, and urchin-like particles through a sequential dissolution–precipitation process, the latter having the best electrochemical performance for lithium-ion batteries.

Orel et al. synthesized Cu_2O nanowires from $Cu(CH_3COO)_2.H_2O$ in di(ethylene glycol) without the addition of surfactant or stabilizer [70]. The nanowires are built with tiny single crystals embedded in an amorphous matrix (Fig. 1.19).

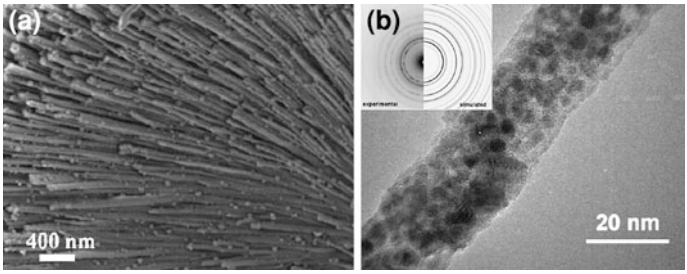

Fig. 1.19 **a** SEM images of Cu_2O nanowires obtained from $Cu(CH_3COO)_2.H_2O$ in di(ethylene glycol) without any additives **b** HRTEM image of Cu_2O nanowire with 2–5 nm crystallites embedded in an amorphous matrix. Inset of b) experimental and simulated SAED patterns [70]

Such a morphology is obtained in a narrow concentration range of the starting acetate under controlled heating and is tentatively explained by the formation of a fibrous glycolate complex which decomposes upon heating leading to Cu_2O retaining the wire-like morphology. Huang et al. controlled the shape of Cu_2O particles by reducing $Cu(CH_3COO)_2.H_2O$ by ethylene glycol with different concentrations of PVP [71]. Nanoparticles prepared without PVP are nanoboxes with an average edge size of 100 nm and a wall thickness of about 20 nm. Nanocubes and nanospheres are obtained at PVP concentrations of 1.0 and 2.0 mM respectively. Whatever their morphology the particles grow by aggregation of smaller single nanocrystals. Previous studies exemplify the potentiality of the polyol process to get nanoparticles of different shapes by using various starting compounds or polyols and by adding a stabilizer at different concentrations.

Several authors reported on modification of shape of zinc oxide nanoparticles. In order to study biocidal effects and cellular internalization of ZnO nanoparticles on *Escherichia coli* bacteria ZnO nanoparticles were synthesized in di(ethylene glycol), particle size and shape being controlled by varying the hydrolysis ratio and/or by addition of small molecules and macromolecules such as tri-n-octylphosphine oxide (TOPO), sodium dodecyl sulfate (SDS), polyoxyethylene stearyl ether (Brij-76), and bovine serum albumin (BSA) [75]. For ZnO prepared without addition of small molecules or macromolecules (Fig. 1.20a), spherical nanoparticles with a broad size distribution were observed. On the other hand, a unique kind of one-dimensionally organized ZnO nanoparticles was obtained by electrostatic stabilization with BSA as templating material (Fig. 1.20b). A very narrow size distribution of ZnO spherical nanoparticles was obtained with addition of TOPO as a template (Fig. 1.20c). In this case, TOPO acts as a template and also as a linker in the self-assembly of ZnO nanoparticles. For ZnO-TOPO synthesis, when hydrolysis ratio increased from $h = 10$ to $h = 30$ and TOPO concentration decreased from 10^{-1} to 10^{-2} M, ZnO nanorods formation was observed (Fig. 1.20d). Finally, ZnO anisotropic morphologies were obtained by coalescence of spherical and cubic nanoparticles in the presence of SDS and

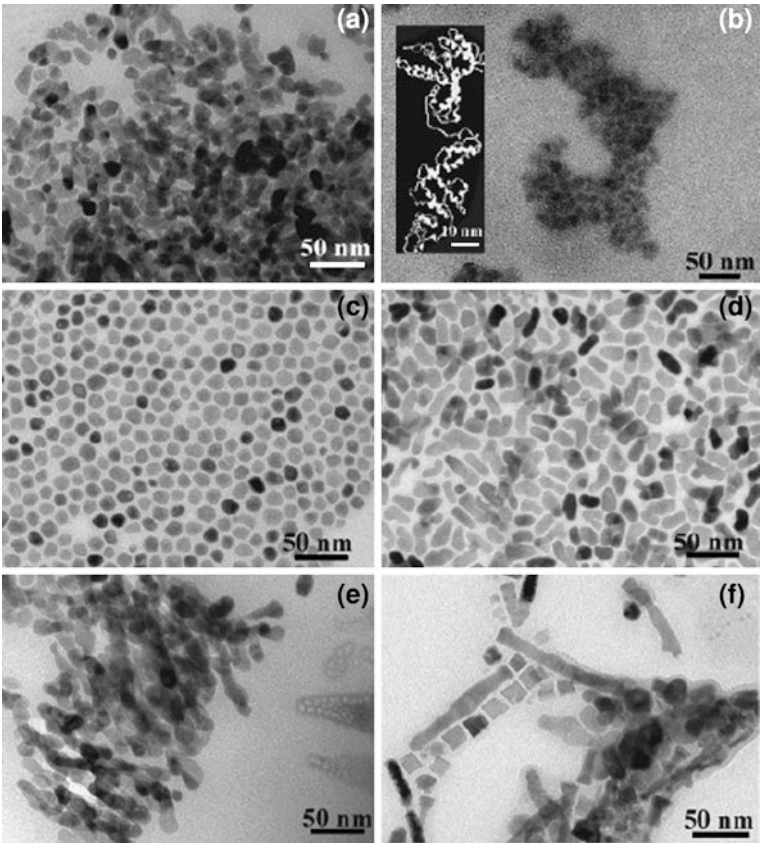

Fig. 1.20 TEM micrographs of ZnO nanoparticles synthesized in DEG medium: **a** ZnO without addition of macromolecules; **b** ZnO-BSA (*top left* schematic BSA conformation); **c** ZnO-TOPO ($h = 10$); **d** ZnO-TOPO ($h = 30$); **e** ZnO-SDS; and **f** ZnO-Brij-76 [75]

Brij-76 macromolecules, respectively (Fig. 1.20e–f). In the case of Brij-76, used as a structure director, assemblies of ZnO nanocubes were observed. These nanocubes have a coalescence tendency that allows formation of ZnO nanobelts (Fig. 1.20f).

By acting upon other synthesis parameters, namely the basicity of the reaction medium, Dakhlaoui et al. synthesized ZnO nanoparticles of various shapes as well. They were obtained from $Zn(CH_3COO)_2.2H_2O$ in di(ethylene glycol) where various amounts of sodium hydroxide were added. When the alkaline ratio ($b = n_{sodium\ \ hydroxide}/n_{metal}$) increases the particles' morphology evolves from anisotropic shape (conical, nanorod-like) to a spherical one [73]. A growth mechanism is proposed on the basis of a selective adsorption of polyol molecules on the non-polar facets and of OH^- ions on the polar {001} ones.

1.4 Conclusion

This chapter provides an overview of an easy to carry out and versatile route to synthesize particulate inorganic materials, the so-called polyol process. It is shown how it is possible to take advantages of the properties of polyols (α-diols and etherglycols), namely their rather high permittivity, their mild reducing power, and their chelating properties, to obtain in such reacting media metal or oxide particles from various inorganic metallic salts and complexes through reduction or hydrolysis reactions. A kinetic control of the nucleation and growth steps allows getting non-agglomerated monodisperse well-crystallized particles. As exemplified by many examples, an accurate and reliable control of the average particle size can be achieved in the nanometer range by modifying experimental parameters or through seeding by foreign nuclei. It is also shown that such a kinetic control allows in certain systems to steer the shape of the particles and namely to induce an anisotropic growth which generates 1D nanostructures such as nanorods or nanowires. This chapter exemplifies the potentiality of the polyol process to tune the size and shape-dependent magnetic properties of ferromagnetic metal or spinel ferrite particles used as advanced functional materials in various fields: high permeability composite materials, high density recording media, high temperature permanent magnets, and biomedical applications such as magnetic resonance imaging, cancer treatment by hyperthermia, or targeted drug delivery.

References

1. US Patent : 4 539 041 (1985) Europe Patent : 0 113 281, 1987
2. Fiévet F, Lagier J-P, Figlarz M (1989) MRS Bull 14:29–34
3. Fiévet F, Lagier J-P, Blin B, Beaudoin B, Figlarz M (1989) Solid State Ion 32(33):l98–205
4. Fiévet F, Fiévet-Vincent F, Lagier J-P, Dumont B, Figlarz M (1993) J Mater Chem 3:627–632
5. Silvert P-Y, Tekaia-Elhsissen K (1995) Solid State Ion 82:53–60
6. Ducamp-Sanguesa C, Herrera-Urbina R, Figlarz M (1993) Solid State Ion 63–65:25–30
7. Ducamp-Sanguesa C, Herrera-Urbina R, Figlarz M (1992) J Solid State Chem 100:272–280
8. Silvert P-Y, Herrera-Urbina R, Duvauchelle N, Vijayakrishnan V, Tekaia-Elhsissen K (1996) J Mater Chem 6:573–577
9. Silvert P-Y, Vijayakrishnan V, Vibert P, Herrera-Urbina R, Tekaia-Elhsissen K (1996) Nanostruct Mater 7:611–618
10. Tekaia-Elhsissen K, Bonet F, Silvert P-Y, Herrera-Urbina R (1999) J Alloy Compd 292:96–99
11. Toneguzzo P, Viau G, Acher O, Fiévet-Vincent F, Fiévet F (1998) Adv Mater 10:1032–1035
12. Viau G, Fiévet-Vincent F, Fiévet F (1996) J Mater Chem 6:1047–1053
13. Toneguzzo P, Viau G, Acher O, Guillet F, Bruneton E, Fiévet-Vincent F, Fiévet F (2000) J Mater Sci 35:3767–3784
14. Jézéquel D, Guenot J, Jouini N, Fiévet F (1995) J Mater Res 10:77–83
15. Feldmann C, Merikhi J (2000) J Colloid Interface Sci 223:229–234
16. Feldmann C, Jungk HO (2001) Angew Chem Int Ed 40:359–362
17. Ammar S, Helfen A, Jouini N, Fiévet F, Villain F, Rosenman I, Danot M, Molinié Ph (2001) J Mater Chem 10:186–192
18. Poul L, Ammar S, Jouini N, Fiévet F, Villain F (2001) Solid State Sci 3:31–42

19. Poul L, Ammar S, Jouini N, Fiévet F, Villain F (2003) J. Sol-Gel Sci Tech 26:261–265
20. Poul L, Jouini N, Fiévet F (2000) Chem Mater 12:3123–3132
21. Feldmann C, Metzmacher C (2001) J Mater Chem 11:2603–2606
22. Antoun T, Brayner R, Al Terary S, Fiévet F, Chehimi M, Yassar A (2007) Eur J Inorg Chem 1275–1284
23. Al Terary S, Mangeney C, Brayner R, Antoun T, Fiévet F, Yassar A (2008) Sens Lett 6:511–517
24. Feldmann C, Jungk H-O (2002) J Mater Sci 37:3251–3254
25. Roming M, Feldmann C (2008) J Mater Sci 43:5504–5507
26. Feldmann C (2003) Adv Funct Mater 13:101–107
27. Wiley B, Sun Y, Mayers B, Xia Y (2005) Chem Eur J 11:454–463
28. Luna C, Morales MP, Serna CJ, Vazquez M (2003) Mater Sci Eng C Biomimetic and Supramol Sys C23(6–8):1129–1132
29. Viau G, Toneguzzo P, Pierrard A, Acher O, Fiévet-Vincent F, Fiévet F (2001) Scripta Mater 44:2263–2267
30. Ung D, Viau G, Fiévet-Vincent F, Herbst F, Richard V, Fiévet F (2005) Prog Solid State Chem 33:137–145
31. Soumare Y, Garcia C, Maurer T, Chaboussant G, Ott F, Fiévet F, Piquemal J-Y, Viau G (2009) Adv Funct Mat 19(12):1971–1977
32. Ung D, Viau G, Ricolleau C, Warmont F, Gredin P, Fiévet F (2005) Adv Mater 17:338–344
33. Sun Y, Gates B, Mayers B, Xia Y (2002) Nano Lett 2:165–168
34. Chkoundali S, Ammar S, Jouini N, Fiévet F, Molinié P, Danot M, Villain F, Grenèche J-M (2004) J Phys Condens Matter 16:4357–4372
35. Ammar S, Jouini N, Fiévet F, Stephan O, Marhic C, Richard M, Villain F, Cartier dit Moulin Ch, Brice S, Sainctavit P (2004) J Non-Crystal Solids 345 and 346:658–662
36. Caruntu D, Remond Y, Chou NH, Jun M-J, Caruntu G, He J, Goloverda G, O'Connor C, Kolesnichenko V (2002) Inorg Chem 41:6137–6146
37. Wang W–W (2008) Mater Chem Phys (2008) 108:227–231
38. Gold SH, Bruce RW, Fliflet AW, Lewis D, Kurihara LK, Imam MA (2007) Rev Sci Instrum 78:023901/1-023901/6
39. Nishioka M, Miyakawa M, Kataoka H, Koda H, Sato K, Suzuki TM (2011) Nanoscale 3:2621–2626
40. LaMer VK, Dinegar RH (1950) J Am Chem Soc 72:4847–4854
41. Viau G, Fiévet-Vincent F, Fiévet F (1996) Solid State Ion 84:259–270
42. Silvert P-Y, Herrera-Urbina R, Tekaia-Elhsissen K (1997) J Mater Chem 7:293–299
43. Joseyphus RJ, Kodama D, Matsumoto T, Sato Y, Jeyadevan B, Tohji K (2007) J Magn Magn Mater 310:2393–2395
44. Joseyphus RJ, Shinoda K, Kodama D, Jeyadevan B (2010) Mater Chem Phys 123:487–493
45. Kodama D, Shinoda K, Sato K, Konno Y, Joseyphus RJ, Motomiya K, Takahashi H, Matsumoto T, Sato Y, Tohji K, Jeyadevan B (2006) Adv Mater 18:3154–3159
46. Takahashi M, Ogawa T, Hasegawa D, Jeyadevan B (2005) J Appl Phys 97:10J307-1-6
47. Dumestre F, Chaudret B, Amiens C, Respaud M, Fejes P, Renaud P, Zurcher P (2003) Angew Chem Int Ed 42:5213–5216
48. Zang Z, Dai S, Blom D, Shen J (2002) Chem Mater 14:965–968
49. Ung D, Soumare Y, Chakroune N, Viau G, Vaulay M-J, Richard V, Fiévet F (2007) Chem Mater 19:2084–2094
50. Maurer T, Ott F, Chaboussant G, Soumare Y, Piquemal J-Y, Viau G (2007) Appl Phys Lett 91:172501
51. Bonet F, Delmas V, Grugeon S, Herrera Urbina R, Silvert P-Y, Tekaia-Elhsissen K (1999) Nanostruct Mater 11:1277–1284
52. Silvert P-Y, Herrera-Urbina R, Tekaia-Elhsissen K (1997) J Mater Chem 7:293–299
53. Viau G, Brayner R, Poul L, Chakroune N, Lacaze E, Fiévet-Vincent F, Fiévet F (2003) Chem Mater 15:486–494
54. Sun Y, Mayers B, Herricks T, Xia Y (2003) Nano Lett 3:955–960
55. Wiley B, Herricks T, Sun Y, Xia Y (2004) Nano Lett 4:1733–1739

56. Korte KE, Skrabalak SE, Xia Y (2008) J Mater Chem 18:437–441
57. Chen J, Herricks T, Geissler M, Xia Y (2004) J Am Chem Soc 126:10854–10855
58. Xiong Y, Chen J, Wiley B, Xia Y (2005) J Am Chem Soc 127:7332–7333
59. Poul L (2000) PhD-Thesis. University Pierre et Marie Curie, Paris, France
60. Jouini N, Poul L, Robert F, Fiévet F (1995) Eur J Solid State Inorg Chem 32:1129–1136
61. Sanchez C, Livage J (1990) New J Chem 14:513–521
62. Ben Tahar L, Smiri LS, Artus M, Joudrier A-L, Herbst F, Vaulay M-J, Ammar S, Fiévet F (2007) Mater Res Bull 42:1888–1896
63. Artus M, Ammar S, Sicard L, Piquemal J-Y, Herbst F, Vaulay M-J, Fiévet F, Richard V (2008) Chem Mater 20:4861–4872
64. Beji Z, Ben Chaabane T, Smiri LS, Ammar S, Fiévet F, Jouini N, Grenèche JM (2006) Phys Stat sol (a) 203:504–512
65. Basti H, Ben Tahar L, Smiri LS, Herbst F, Vaulay M-J, Chau F, Ammar S, Benderbous S (2010) J Colloid Interface Sci 341:248–254
66. Basti H (2010) PhD-Thesis. University Paris Diderot, Paris, France
67. Beji Z, Hanini A, Smiri LS, Gavard J, Kacem K, Villain F, Grenèche J-M, Chau F, Ammar S (2010) Chem Mater 22:5420–5429
68. Ammar S, Jouini N, Fiévet F, Beji Z, Smiri L, Molinié P, Danot M, Grenèche JM (2006) J Phys Condens Mater 18:9055–9069
69. Grugeon S, Laruelle S, Herrera-Urbina R, Dupont L, Poizot P, Tarascon J-M (2001) J Electrochem Soc 148:A285–A292
70. Orel ZC, Anzlovar A, Drazic G, Zigon M (2007) Cryst Growth Des 7:453–458
71. Huang L, Peng F, Yu H, Wang H (2008) Mater Res Bull 43:3047–3053
72. Park JC, Kim J, Kwon H, Song H (2009) Adv Mater 21:803–807
73. Dakhlaoui A, Jendoubi M, Smiri LS, Kanaev A, Jouini N (2009) J Cryst Growth 311: 3989–3996
74. Wan J, Cai W, Meng X, Liu E (2007) Chem Commun 47:5004–5006
75. Brayner R, Ferrari-Iliou R, Brivois N, Djediat S, Benedetti M, Fiévet F (2006) Nano Lett 6:866–870